

Topological quantum control: Edge currents via Floquet depinning of skyrmions in the $\nu = 0$ graphene quantum Hall antiferromagnet

Deepak Iyer¹ and Matthew S. Foster^{2,3}

¹*Department of Physics & Astronomy, Bucknell University, Lewisburg, Pennsylvania 17837, USA*

²*Department of Physics and Astronomy, Rice University, Houston, Texas 77005, USA*

³*Rice Center for Quantum Materials, Rice University, Houston, Texas 77005, USA*

(Dated: March 17, 2020)

We propose a defect-to-edge topological quantum quench protocol that can efficiently inject electric charge from defect-core states into a chiral edge current of an induced Chern insulator. The initial state of the system is assumed to be a Mott insulator, with electrons bound to topological defects that are pinned by disorder. We show that a “critical quench” to a Chern insulator mass of order the Mott gap shunts charge from defects to the edge, while a second stronger quench can trap it there and boost the edge velocity, creating a controllable current. We apply this idea to a skyrmion charge in the $\nu = 0$ quantum Hall antiferromagnet in graphene, where the quench into the Chern insulator could be accomplished via Floquet driving with circularly polarized light.

The pervasive emphasis on topology in modern condensed matter physics is due to two seemingly disparate pursuits. On one hand, topology can “protect” interesting quantum phenomena against imperfections or environmental decoherence, enabling ballistic propagation through edge states [1–3], and quantum information storage and manipulation [4]. On the other hand, topological defects (solitons and instantons [5]) in effective quantum field theories play a central role in non-perturbative frameworks for strongly correlated electron systems [6, 7]. In particular, topological defects in bosonic order parameters can bind fermion quasiparticles in their cores; the topological charge of the defect then determines the ground-state electrical charge or current induced by it [8–10]. Applications of this principle in condensed matter physics range from producing fractionally charged zero modes in graphene [11], to novel mechanisms for superconductivity [12] and quantum criticality [13–16].

In this Letter, we combine these two notions of topology in a dynamical setting, using a quantum quench. We consider a quench into a 2D Chern insulator (Haldane) phase [1], with dynamically generated edge states in a honeycomb model with Dirac fermions. Previous work considered quenches from spatially homogeneous, trivial or topological initial states [17–24]. Here, we instead envision an antiferromagnetic (Néel-ordered) Mott insulating initial state, wherein topological skyrmion defects trap Dirac electrons or holes in their cores [9, 10, 12, 15, 16, 25]. The skyrmion defects are initially pinned by disorder, providing a robust reservoir of localized charge for a weakly-doped initial Mott insulating state. We subject the Mott state to a quenching on of the Chern insulator mass, which competes with the Néel order. We find that a “critical” quench can efficiently transfer the charge bound to a skyrmion defect to the quench-induced chiral edge states formed at the boundary of the sample. Here, a critical quench means that the induced Haldane mass is tuned to match the ground state Mott gap. After transferring the charge to the edge, a second quench deeper

into the Haldane phase traps the charge at the sample boundary, inducing a tunable circulating edge current. Thus our double-quench protocol provides a way to efficiently depin electric charge from topological defects of the Mott reservoir and transfer it to the boundary of a dynamically-induced topological insulator.

Our protocol could be implemented using Floquet driving with circularly polarized light in graphene [26, 27], as explicated in Fig. 1. Many theoretical works have examined Floquet-induced Chern insulator states that could be realized in semimetallic graphene, with proposals to measure induced topological edge states through conducting leads [26–30]. However, even in the ideal case of ballistic Landauer transmission through such a driven de-

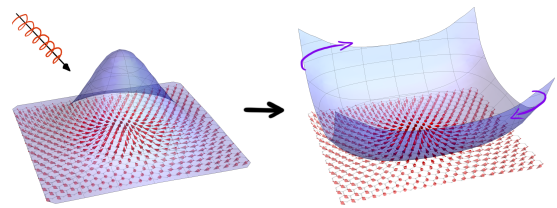


FIG. 1. A topological quantum control protocol for creating chiral edge currents. A Chern insulating (Haldane) mass is induced by the application of circularly polarized light [26–32], incident on Mott-insulating graphene with a single skyrmion embedded in a Néel antiferromagnetic texture. A single hole is doped into the negative-energy core state bound to the skyrmion [9, 10, 15, 16]. Such a defect can arise as a pinned charge carrier in the $\nu = 0$ quantum Hall state of graphene [33–36]. When the strength of the incident light is at criticality (with respect to the topological transition induced by a Haldane mass), the doped hole ballistically migrates to the edge of the sample. A second quench (not shown) deep into the topological phase sets up a circulating current of the charge, as indicated by the purple arrows. The spins show the skyrmion texture on the underlying honeycomb lattice and the blue surface illustrates the charge density. For weak and moderate quenches, the spin texture in our mean-field calculation is not significantly scrambled.

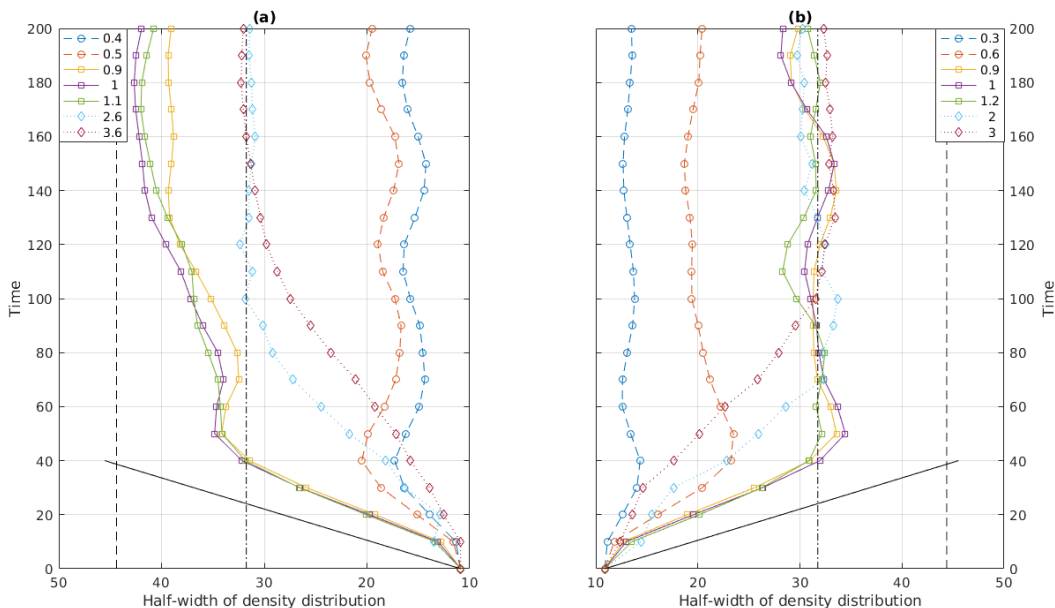


FIG. 2. Half-width (standard deviation) of the electric charge distribution around the center of the skyrmion texture as a function of time. A single hole is doped into the negative-energy core state of the skyrmion defect in a Néel background before the quench. This hole is “depinned” by the quenching on of a competing mass (order parameter). (a) corresponds to a quench into the Chern insulating phase of the Haldane model, and (b) corresponds to a quench into a model with a sublattice-staggered mass [charge density wave (CDW) order] that displays no topologically nontrivial phase. The legend indicates values of the quench coupling strength normalized so that the equilibrium gap (with coexisting Néel and Chern insulator or CDW orders) closes at unity: for (a) it is $3\sqrt{3}t_2/m_N$ and for (b) m_C/m_N . Here t_2 (m_C) is the Haldane hopping (CDW) strength, and m_N is the energy gap in the homogeneous Néel background. In both figures, the solid black line represents the light-cone given by the Fermi velocity, $v_F = \sqrt{3}t/2$, the black dash-dot line represents the value of the half-width for a uniform charge distribution across the graphene flake, and the black dashed line represents the value for all charge concentrated on the edge. As the strength of the Haldane coupling t_2 increases, the initial charge density profile spreads faster and faster until the gap closes, after which the spreading slows down. Note that curves with values of the half-width greater than the uniform value (black dot-dash line) have greater charge density on the edge/boundary of the sample than the bulk. Near criticality in (a), edge states are strongly populated, and expansion is nearly ballistic (modulo boundary effects and a slow start) at the Fermi velocity. However, we do not see any corresponding shift of charge to the edge in the CDW case due to the absence of topologically nontrivial edge states in (b). Thus, there is a nontrivial effect from pumping the sample with circularly polarized light to create the Haldane mass (a).

vice, the complicated matching conditions between time-dependent device and equilibrium contact states typically leads to the prediction of a non-quantized response in transport [28–30]. Since the Dirac point conductivity of graphene itself is always of order e^2/h at low temperature [37], the transition to almost-quantized edge transport is not easy to verify in a two-terminal Landauer geometry. Transport measurements typically require long averaging times, while steady-state illumination on ungapped graphene can excite many hot electron-hole carriers. Then, it becomes essential to model the distribution function of the electrons induced by the drive [31], which goes beyond the Floquet-Landauer theory. Ultrafast pumping and detection can mitigate these limitations, see Ref. [32] for a recent experiment.

In this Letter, we instead propose to apply a circularly-polarized Floquet drive to the *strongly insulating* $\nu = 0$

quantum Hall state of graphene [38, 39]. The insulating gap in the $\nu = 0$ state arises due to quantum Hall magnetism [40] in the nearly $SU(4)$ -symmetric zeroth lowest Landau level (LLL) [41–43]. Due to the LLL projection, the charge carriers in quantum Hall magnets typically exhibit a topological skyrmion texture in the magnetic order [40, 44, 45]. This $\nu = 0$ state in graphene has only recently been understood as a quantum Hall *antiferromagnet* (AFM) in physical spin [33–35], which should support $SU(2)$ skyrmion charge excitations [36, 43]. A similar setup could start with Mott states in twisted bilayer graphene systems [46–48].

When a quantum Hall magnet is doped very slightly away from integer filling, skyrmionic charge carriers are expected to be pinned randomly throughout the sample by weak quenched disorder [40]. We model the $\nu = 0$ state of graphene using a honeycomb lattice model sub-

ject to mean-field Néel antiferromagnetism, with a single skyrmion defect localized in the center of a finite square sample (with open boundary conditions). The defect traps a single pair of subgap, positive and negative-energy core states. The core states form a particle-hole-symmetric pair in the K and K' valleys [15]. We consider a system tuned just below half-filling, with the negative-energy core occupied by a hole. The Floquet drive is treated as an instantaneous quantum quench that turns on the Haldane Chern insulator mass [19, 21–24], an approximation [27] that becomes exact in the high-frequency limit [49, 50].

We show that a quench of critical strength (matching the dynamically generated Haldane and ground-state AFM mass gaps) depins the doped hole, which ballistically propagates to edge. To demonstrate that this effect is a nontrivial consequence of the Chern mass quench, we show that a similar “sticking” of the depinned charge to the sample boundary does not occur for a quench employing the topologically trivial charge density wave mass; see Figs. 2 and 3. Finally, we show that a second quench that intensifies the Haldane mass can trap the migrated charge at the boundary of the sample for a long time, inducing a circulating electrical current with an edge velocity determined by the drive strength (Fig. 4). The key new ingredient in our nonequilibrium scheme is that we controllably induce and populate the edge states, depinning charges from topological defects in a strongly insulating prequench state.

Model.—We consider spin-1/2 electrons hopping on a honeycomb lattice, subject to an inhomogeneous, sublattice-staggered Zeeman field that mimics a skyrmion defect texture in the Néel background. The prequench Hamiltonian is given by

$$H_{\text{sk}} = -t \sum_{\alpha} \sum_{r,s} (c_{r,\alpha}^{\dagger} c_{r+s,\alpha} + \text{H.c.}) + m_N \sum_r (-1)^{\tau} \vec{n}(r) \cdot c_{r,\alpha}^{\dagger} \vec{\sigma}^{\alpha\beta} c_{r,\beta}. \quad (1)$$

The first term encodes nearest-neighbor hopping; H.c. denotes the Hermitian conjugate. The second term is the Zeeman coupling, where τ is 0 for $r \in A$ and 1 for $r \in B$ (A, B denote the sublattices). Here α is the spin index, and $\vec{\sigma}$ is a vector formed from the Pauli matrices acting on physical spin.

In Eq. (1), we choose $\vec{n}(r)$ to be a skyrmion texture in the continuum [5]. On the lattice, we superimpose this onto the vertices with the skyrmion centered on a plaquette at the center of the lattice. The texture is parameterized by $\omega(z) \equiv z/\lambda$, where λ is a scale that determines the core size, and $z = x + iy$. The spin texture is given by $n_z = (|\omega|^2 - 1) / (|\omega|^2 + 1)$, $n_x + in_y = (2\omega) / (|\omega|^2 + 1)$. For $|z| \gg \lambda$ and $|z| \ll \lambda$, the texture becomes uniform and points in the $\pm z$ direction (i.e., out of the graphene plane) and is essentially a homogeneous Néel mass, m_N .

This Hamiltonian has a nonzero gap, and a particle-hole symmetric pair of positive- and negative-energy bound states, localized to the skyrmion core [15, 16]. The spin textures of the core states wind like the original skyrmion texture shown in Fig. 1, since the Zeeman term pins the spin orientation. Each core state can accommodate a single electron charge; the skyrmion carries unit topological or Pontryagin charge [5, 34]. We fill all the states at negative energy, *except* for the negative-energy core state (which is doped with a hole). Equivalently, we could fill all negative energy states and the positive-energy core state. The ground-state density profile reflects the missing charge bound to the core state. By contrast, at half filling, the charge density would be uniform.

The quantum quench evolves this initial state with an additional Haldane term, $H = H_{\text{sk}} + H_H$, where

$$H_H = it_2 \sum_{\alpha} \sum_{r,s \in \{\text{nnn}\}} c_{r,\alpha}^{\dagger} c_{r+s,\alpha} + \text{H.c.}, \quad (2)$$

such that the positive signs form counterclockwise triangles in each sublattice [1]. In order to correlate any unique behavior that emerges from quenching into a topologically nontrivial phase, we also carry out a quench where we turn on a topologically trivial charge density wave (CDW) potential (equivalently, a sublattice-staggered mass), $H = H_{\text{sk}} + H_C$, where

$$H_C = m_C \sum_{r,\alpha} (-1)^{\tau} c_{r,\alpha}^{\dagger} c_{r,\alpha}. \quad (3)$$

Here, as before, $\tau = \{0, 1\}$ for $r \in \{A, B\}$ respectively. All states of this model are topologically trivial. In particular, there are no current-carrying edge states. Both the Chern-insulator and CDW terms compete with the Néel order; sufficiently large t_2 or m_C relative to m_N can close the bulk gap in equilibrium. We note that in a finite sample as studied numerically here, both models $H = H_{\text{sk}} + H_{H,C}$ show edge states *near gap closure* coming from the open boundary conditions.

Numerics.—In equilibrium, the model with a homogeneous Néel mass undergoes a quantum phase transition at $m_N = 3\sqrt{3}t_2$, at which point the gap closes, and edge states appear [1]. As t_2 increases beyond this value, a gap reappears. However, edge states that connect across the gap persist. For the model with the skyrmion texture, we observe that the gap closes at approximately the same point [see inset, Fig. 3(a)], with the subtlety that the two skyrmion-core bound states are present almost until the gap closes. We tune the quench through this quantum phase transition and study the resulting evolution of the charge density and charge current. Since the Haldane term is diagonal in spin, we do not expect any nontrivial behavior in the spin sector. We perform calculations on a square-shaped section of the honeycomb lattice, with two zigzag edges and two armchair edges using numerical exact diagonalization on a lattice 82 plaquettes wide.

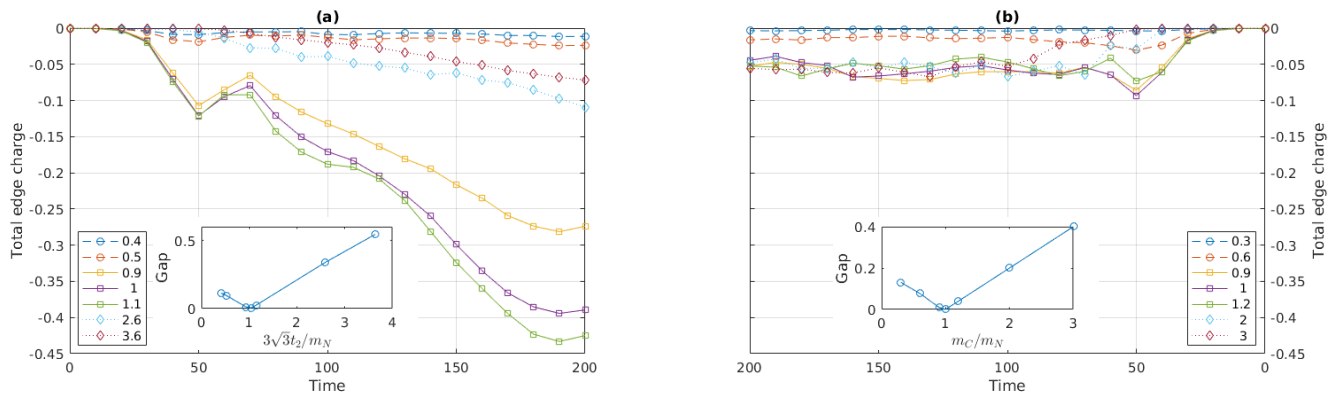


FIG. 3. Total charge on the boundary (measured relative to the half-filled background) following the same quench pictured in Fig. 2. (a) corresponds to the case when we quench into the Haldane model, (b) the quench into a topologically trivial CDW model. Legends indicate the relevant quench parameter (see Fig. 2). In (b), we see no significant motion of charge to the boundary, whereas in the Haldane model (a), almost half of the total charge has moved to the boundary (see black dashed line). Here, we compute the charge at the very edge of the sample. If we include a thicker boundary layer, then we capture most of the electric charge initially bound to the skyrmion-core. In both cases, far from the critical point, we don't see significant motion of charge to the boundary. Insets in each figure show the equilibrium gaps as a function of the relevant tuning parameter.

The specific shape of the flake is irrelevant since our initial spatially inhomogeneous Hamiltonian breaks lattice symmetries.

Charge dynamics.—The first observation and primary result is the rapid population of the edge of the sample near criticality. The skyrmion-core (hole) charge density starts out near the center of the sample, but rapidly moves outwards, as seen in Figs. 2 and 3. In Fig. 2, the radial spread of the charge density (standard deviation) is plotted against time for different values of the Haldane mass t_2 . Away from the critical point, $3\sqrt{3}t_2/m_N \approx 1$, the spreading is slow. In the weak-quench regime, this is because of the absence of edge states and a nonzero gap. In the strong-quench regime, edge states are present but have weak overlap with the initial state. It is only near criticality, i.e. where the gap closes and edge states appear, that we get rapid charge accumulation at the edge. The small gap between the bulk-core and edge states promotes efficient hybridization between these. It is nevertheless interesting to note that the charge density preferentially occupies the edge as opposed to a more uniform distribution. As the system continues to evolve in time, we observe a slow relaxation.

In comparison, as seen in Figs. 2(b) and 3(b), the topologically trivial CDW quench does not produce the saturation of charge at the sample boundary that we see in the Haldane quench. Although there are no topologically protected chiral edge states in this case, almost degenerate edge states nevertheless exist on account of the finite sample and appear at gap closure at $m_N = m_C$ [in equilibrium, see inset, Fig 3(b)]. In spite of this, we do not see significant population of these edge states, indicating that the topologically nontrivial nature of edge states

that appear when we shine circularly polarized light play a key role in the effect we observe.

Edge currents.—The edge states of the Haldane model show nontrivial currents circulating around the sample in the topological phase, their sense depending on the sign of t_2 [1]. We therefore expect to see a circulating edge charge when we quench into the topological phase, since the charge initially bound to the skyrmion is pushed out to the edge.

In the equilibrium model, strong edge currents appear deep in the topological phase. When we quench on the Haldane coupling, charge rushes to the boundary only near criticality. However, near criticality, the edge currents are not strong (owing in part to the shallow edge velocity). Deeper in the topological phase, the edge velocity is enhanced and edge currents are strong; however, a direct deep quench does not shift significant charge to the boundary.

In order to generate a strong edge current, we therefore adopt a *double quench* protocol, see Fig. 4(a). The first quench shifts the charge to the edge, and the second quench strongly confines this charge and induces circulation with finite velocity [see inset, Fig. 4(a)]. We illustrate this effect in Fig. 4(b). The large figure shows a single temporal snapshot as an illustration. The plot itself represents the current flowing in each bond between the lattice sites. The blown-up images show snapshots at increasing time after the second quench (the first quench is allowed to evolve until we maximize the edge charge). Note how the current shifts to the right i.e., a clockwise flow. The arrows in each snapshot are opposite to the overall flow since this is a hole current. Applying the double-quench protocol to a sample with a finite density

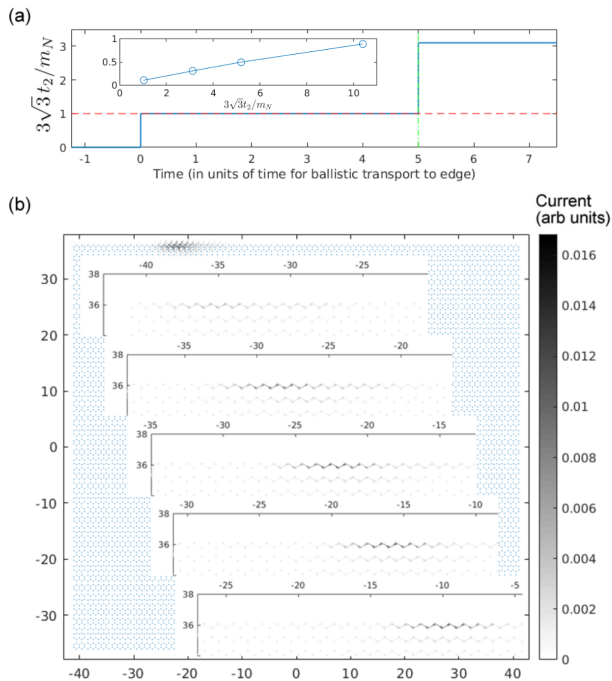


FIG. 4. Edge currents induced by a double quench. The double-quench protocol is shown in (a), the currents in (b). The inset in (a) shows the average edge velocity as a function of the Haldane mass after the second quench, in units of the lattice parameter \times hopping energy; the blue line is a guide to the eye. The edge velocity increases with increasing strength of the second quench, allowing control of the induced edge current. The enlarged snapshots in (b) indicate time evolution going down along the images. The current shifts towards the right as time evolves (note horizontal axis). In each snapshot, the arrows point in the direction of the charge current; charge and particle currents are opposite for the edge-migrated hole. The background image shows the full sample at a particular time snapshot. Note that there is almost no current anywhere else in the sample. The scale on the right indicates the value of the current.

of hole-doped skyrmions would trap a finite proportion of the core charge at the boundary, with the second quench producing a tunable, steady-state edge current.

Conclusion.—Charges pinned to topological defects in a Mott insulator can serve as a charge reservoir that can be utilized to efficiently load chiral edge states in a quantum-quench induced Chern insulator, producing a tunable circulating edge current. Such a quench could be simulated in the $\nu = 0$ quantum Hall antiferromagnetic state in graphene [33–36, 43], using a Floquet drive [26, 27]. Future work could apply the same strategy to twisted bilayer Mott states [46–48].

The induced edge current predicted here could be measured via the laser-triggered photoconductive switch technique employed in the experiment [32]. Alternatively, it might be possible to perform an all-optical measurement of the THz light re-emitted by a sufficiently

large edge current induced by an intense THz pulse.

We thank Junichiro Kono and Chia-Chuan Liu for useful discussions. We thank Yunxiang Liao for a collaboration on a precursor to this work. This work was supported by U.S. Army Research Office Grant No. W911NF-17-1-0259, and by NSF CAREER Grant No. DMR-1552327. D.I. is grateful to the Rice Center of Quantum Materials for its hospitality during various states of this work.

- [1] F. D. M. Haldane, Model for a Quantum Hall Effect without Landau Levels: Condensed-Matter Realization of the “Parity Anomaly,” *Phys. Rev. Lett.* **61**, 2015 (1988).
- [2] Z. M. Hasan and C. L. Kane, Colloquium: Topological insulators, *Rev. Mod. Phys.* **82**, 3045 (2010).
- [3] B. A. Bernevig and T. L. Hughes, *Topological Insulators and Topological Superconductors* (Princeton University Press, Princeton, New Jersey, 2013).
- [4] C. Nayak, S. H. Simon, A. Stern, M. Freedman, and S. Das Sarma, Non-Abelian anyons and topological quantum computation, *Rev. Mod. Phys.* **80**, 1083 (2008).
- [5] R. Rajaraman, *Solitons and Instantons: An Introduction to Solitons and Instantons in Quantum Field Theory* (North-Holland, Amsterdam, Netherlands 1982).
- [6] E. Fradkin, *Field Theories of Condensed Matter Physics*, 2nd ed. (Cambridge University Press, Cambridge, England 2013).
- [7] A. Altland and B. D. Simons, *Condensed Matter Field Theory*, 2nd ed. (Cambridge University Press, Cambridge, England 2010).
- [8] J. Goldstone and F. Wilczek, Fractional Quantum Numbers on Solitons, *Phys. Rev. Lett.* **47**, 986 (1981).
- [9] T. Jaroszewicz, Induced Fermion Current in the σ Model in (2+1) Dimensions, *Phys. Lett.* **146B**, 337 (1984).
- [10] M. Carena, S. Chaudhuri, and C. E. M. Wagner, Induced fermion number in the O(3) nonlinear σ model, *Phys. Rev. D* **42**, 2120 (1990).
- [11] C.-Y. Hou, C. Chamon, and C. Mudry, Electron Fractionalization in Two-Dimensional Graphenelike Structures, *Phys. Rev. Lett.* **98**, 186809 (2007).
- [12] T. Grover and T. Senthil, Topological Spin Hall States, Charged Skyrmions, and Superconductivity in Two Dimensions, *Phys. Rev. Lett.* **100**, 156804 (2008).
- [13] A. Tanaka and X. Hu, Many-Body Spin Berry Phases Emerging from the π -Flux State: Competition between Antiferromagnetism and the Valence-Bond-Solid State, *Phys. Rev. Lett.* **95**, 036402 (2005).
- [14] L. Fu, S. Sachdev, and C. Xu, Geometric phases and competing orders in two dimensions, *Phys. Rev. B* **83**, 165123 (2011).
- [15] P. Goswami and Q. Si, Topological defects of Néel order and Kondo singlet formation for the Kondo-Heisenberg model on the honeycomb lattice, *Phys. Rev. B* **89**, 045124 (2014).
- [16] C.-C. Liu, P. Goswami, and Q. Si, Skyrmion defects and competing singlet orders in a half-filled antiferromagnetic Kondo-Heisenberg model on the honeycomb lattice, *Phys. Rev. B* **96**, 125101 (2017).
- [17] M. S. Foster, M. Dzero, V. Gurarie, and E. A.

- Yuzbashyan, Quantum quench in a $p + ip$ superfluid: Winding numbers and topological states far from equilibrium, *Phys. Rev. B* **88**, 104511 (2013).
- [18] M. S. Foster, V. Gurarie, M. Dzero, and E. A. Yuzbashyan, Quench-Induced Floquet Topological p -Wave Superfluids, *Phys. Rev. Lett.* **113**, 076403 (2014).
- [19] L. D'Alessio and M. Rigol, Dynamical preparation of Floquet Chern insulators, *Nat. Comm.* **6**, 8336 (2015).
- [20] Y. Liao and M. S. Foster, Spectroscopic probes of isolated nonequilibrium quantum matter: Quantum quenches, Floquet states, and distribution functions, *Phys. Rev. A* **92**, 053620 (2015).
- [21] M. D. Caio, N. R. Cooper, and M. J. Bhaseen, Quantum Quenches in Chern Insulators, *Phys. Rev. Lett.* **115**, 236403 (2015).
- [22] P. Wang and S. Kehrein, Phase transitions in the diagonal ensemble of two-band Chern insulators, *New J. Phys.* **18**, 053003 (2016).
- [23] M. D. Caio, N. R. Cooper, and M. J. Bhaseen, Hall response and edge current dynamics in Chern insulators out of equilibrium, *Phys. Rev. B* **94**, 155104 (2016).
- [24] S.-F. Liou and K. Yang, Quench dynamics across topological quantum phase transitions, *Phys. Rev. B* **97**, 235144 (2008).
- [25] I. F. Herbut, C.-K. Lu, and B. Roy, Conserved charges of order-parameter textures in Dirac systems, *Phys. Rev. B* **86**, 075101 (2012).
- [26] T. Oka and H. Aoki, Photovoltaic Hall effect in graphene, *Phys. Rev. B* **79**, 081406 (2009); Erratum: Photovoltaic Hall effect in graphene [Phys. Rev. B 79, 081406(R) (2009)], *Phys. Rev. B* **79**, 169901 (2009).
- [27] T. Kitagawa, T. Oka, A. Brataas, L. Fu, and E. Demler, Transport properties of nonequilibrium systems under the application of light: Photoinduced quantum Hall insulators without Landau levels, *Phys. Rev. B* **84**, 235108 (2011).
- [28] Z. Gu, H. A. Fertig, D. P. Arovas, and A. Auerbach, Floquet spectrum and Transport through an Irradiated Graphene Ribbon, *Phys. Rev. Lett.* **107**, 216601 (2011).
- [29] A. Kundu, H. A. Fertig, and B. Seradjeh, Effective Theory of Floquet Topological Transitions, *Phys. Rev. Lett.* **113**, 236803 (2014).
- [30] L. E. F. Foa Torres, P. M. Perez-Piskunow, C. A. Balseiro, and G. Usaj, Multiterminal Conductance of a Floquet Topological Insulator, *Phys. Rev. Lett.* **113**, 266801 (2014).
- [31] H. Dehghani, T. Oka, and A. Mitra, Out-of-equilibrium electrons and the Hall conductance of a Floquet topological insulator, *Phys. Rev. B* **91**, 155422 (2015).
- [32] J. W. McIver, B. Schulte, F.-U. Stein, T. Matsuyama, G. Jotzu, G. Meier, and A. Cavalleri, Light-induced anomalous Hall effect in graphene, *Nat. Phys.* **16**, 38 (2020).
- [33] J. Jung and A. H. MacDonald, Theory of the magnetic-field-induced insulator in neutral graphene sheets, *Phys. Rev. B* **80**, 235417 (2009).
- [34] M. Kharitonov, Phase diagram for the $\nu = 0$ quantum Hall state in monolayer graphene, *Phys. Rev. B* **85**, 155439 (2012).
- [35] A. F. Young, J. D. Sanchez-Yamagishi, B. Hunt, S. H. Choi, K. Watanabe, T. Taniguchi, R. C. Ashoori, and P. Jarillo-Herrero, Tunable symmetry breaking and helical edge transport in a graphene quantum spin Hall state, *Nature* **505**, 528 (2014).
- [36] T. Jolicoeur and B. Pandey, Quantum Hall skyrmions at $\nu = 0, \pm 1$ in monolayer graphene, *Phys. Rev. B* **100**, 115422 (2019).
- [37] S. Das Sarma, S. Adam, E. H. Hwang, and E. Rossi, Electronic transport in two-dimensional graphene, *Rev. Mod. Phys.* **83**, 407 (2011).
- [38] J. G. Checkelsky, L. Li, and N. P. Ong, Zero-Energy State in Graphene in a High Magnetic Field, *Phys. Rev. Lett.* **100**, 206801 (2008).
- [39] A. F. Young, C. R. Dean, L. Wang, H. Ren, P. Cadden-Zimansky, K. Watanabe, T. Taniguchi, J. Hone, K. L. Shepard, and P. Kim, Spin and valley quantum Hall ferromagnetism in graphene, *Nat. Phys.* **8**, 550 (2012).
- [40] S. M. Girvin, The Quantum Hall Effect: Novel Excitations and Broken Symmetries, in *Topological aspects of low dimensional systems*, edited by A. Comtet, T. and Jolicoeur, S. Ouvry, and F. David (Springer, Berlin, Germany 1999).
- [41] D. A. Abanin, P. A. Lee, and L. S. Levitov, Spin-Filtered Edge States and Quantum Hall Effect in Graphene, *Phys. Rev. Lett.* **96**, 176803 (2006).
- [42] K. Nomura and A. H. MacDonald, Quantum Hall Ferromagnetism in Graphene *Phys. Rev. Lett.* **96**, 256602 (2006).
- [43] K. Yang, S. Das Sarma, and A. H. MacDonald, Collective modes and skyrmion excitations in graphene $SU(4)$ quantum Hall ferromagnets, *Phys. Rev. B* **74**, 075423 (2006).
- [44] S. L. Sondhi, A. Karlhede, S. A. Kivelson, and E. H. Rezayi, Skyrmions and the crossover from the integer to fractional quantum Hall effect at small Zeeman energies, *Phys. Rev. B* **47**, 16419 (1993).
- [45] D. P. Arovas, A. Karlhede, and D. Lilliehöök, $SU(N)$ quantum Hall skyrmions, *Phys. Rev. B* **59**, 13147 (1999).
- [46] Y. Cao, V. Fatemi, A. Demir, S. Fang, S. L. Tomarken, J. Y. Luo, J. D. Sanchez-Yamagishi, K. Watanabe, T. Taniguchi, E. Kaxiras, R. C. Ashoori, and P. Jarillo-Herrero, Correlated insulator behaviour at half-filling in magic-angle graphene superlattices, *Nature* **556**, 80 (2018).
- [47] X. Lu, P. Stepanov, W. Yang, M. Xie, M. A. Aamir, I. Das, C. Urgell, K. Watanabe, T. Taniguchi, G. Zhang, A. Bachtold, A. H. MacDonald, and D. K. Efetov, Superconductors, orbital magnets and correlated states in magic-angle bilayer graphene, *Nature* **574**, 653 (2019).
- [48] A. L. Sharpe, E. J. Fox, A. W. Barnard, J. Finney, K. Watanabe, T. Taniguchi, M. A. Kastner, and D. Goldhaber-Gordon, Emergent ferromagnetism near three-quarters filling in twisted bilayer graphene, *Science* **365**, 605 (2019).
- [49] W. Magnus, On the exponential solution of differential equations for a linear operator, *Commun. Pur. Appl. Math.* **7**, 649 (1954).
- [50] F. Casas, J. A. Oteo, and J. Ros, Floquet theory: exponential perturbative treatment, *J. Phys. A-Math. Theor.* **34**, 3379 (2001).